

# INTERNATIONAL SOCIETY FOR SOIL MECHANICS AND GEOTECHNICAL ENGINEERING



*This paper was downloaded from the Online Library of the International Society for Soil Mechanics and Geotechnical Engineering (ISSMGE). The library is available here:*

<https://www.issmge.org/publications/online-library>

*This is an open-access database that archives thousands of papers published under the Auspices of the ISSMGE and maintained by the Innovation and Development Committee of ISSMGE.*

# 2D base stability evaluation of excavations in soft soils by FE analysis

Toshiyuki Hagiwara  
Nishimatsu Construction Co. Ltd., Japan

Hamdy Faheem, Fei Cai, Keizo Ugai  
Department of Civil Engineering, Gunma University, Japan

**ABSTRACT:** The two-dimensional base stability of excavations is evaluated using the finite element method with reduced shear strength. The numerical results indicate that the base stability of excavations is significantly influenced by the ratio of the depth to the width of the excavations, the thickness of the soft soil layer between the excavation base and hard stratum, the embedded length of the walls, and the stiffness of the walls around the excavation.

## 1 INTRODUCTION

Evaluation of the safety factor against base instability is important in the design of excavations in soft soils. The undrained condition usually governs the stability of an excavation immediately after construction, and a total stress analysis is pertinent. Several limit equilibrium methods are available for evaluating the base stability of excavations. The calculated safety factors vary with different methods. Up to the present, the safety factor of excavations has been usually predicted using the methods proposed by Terzaghi (1943) or Bjerrum & Eide (1956). However, Terzaghi's method is only used for shallow or wide excavation with  $H/B \leq 1.0$ , where  $B$  and  $H$  are the width and depth of the excavation, respectively, as shown in Figure 1. For Bjerrum & Eide's method, some modification to the  $N_c$ -values is necessary when a hard stratum is present near the excavation base. This is because the failure surface will not extend fully across the base of the excavation, and a deep foundation failure mode is no longer realistic.

The above-mentioned two methods were developed before the introduction of stiffer retaining wall systems such as diaphragm walls and secant piles. Hence, the safety factors given by these methods do not consider the stiffness,  $EI$ , of the wall and the embedded length of the wall below the excavation base,  $D$ . In this study, the finite element method with reduced shear strength is used to evaluate the two-dimensional base stability of excavations. The influences of  $H/B$ , the clay thickness under the base of excavation,  $T$ , the wall stiffness,  $EI$ , the embedded length of the wall,  $D$ , and the net distance between the end of the wall and the hard stratum,  $T_n$ , have

been considered on the base stability. The effects of strain softening and anisotropy have not been considered in the finite element method as in the limit equilibrium method.

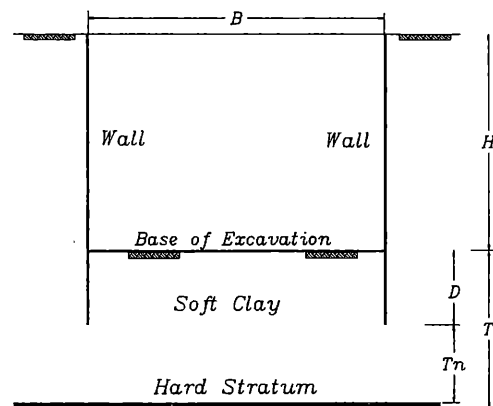


Figure 1. Geometry of braced excavation.

## 2 FEM WITH REDUCED SHEAR STRENGTH

The FEM with reduced shear strength has been gradually used to analyze the slope stability in two-dimensional situations (e.g. Zienkiewicz et al. 1975, Ugai 1989, Matsui & San 1992, Griffiths & Lane 1999), and three-dimensional situations (Ugai & Leshchinsky 1995, Cai & Ugai 2000). The safety factor is evaluated by the gradual reduction of the shear strength parameters ( $c$ ,  $\phi$ ) of the soil inducing the divergence (failure) of the nonlinear analysis, where the shear strength equation is  $\tau_f = c' + \sigma' \tan \phi'$ . The reduced shear strength pa-

parameters  $c'_F$  and  $\phi'_F$  will replace the corresponding values of  $c'$  and  $\phi'$  in the above equation to  $c'_F = c'/F$  and  $\phi'_F = \tan^{-1}(\tan(\phi')/F)$ . So the equation with reduced shear strength can be written as  $\tau_{fF} = c'_F + \sigma' \tan \phi'_F$ .

The initial value of  $F$  is assumed to be sufficiently small so as to produce a nearly elastic problem. Then the value of  $F$  is increased step by step until finally a global failure develops (Ugai & Leshchinsky 1995). The load step is controlled by the increment of the safety factor. If convergence cannot be reached after for example, 1000 iterations, the value of  $F$  just before this load step is taken to be unique safety factor  $F_s$ . This method is called the shear strength reduction FEM (SSRFEM).

The details of the FEM with reduced shear strength can be found in Cai & Ugai (2000). The numerical comparisons have shown that the FEM with reduced shear strength is a reliable and robust method for assessing the safety factor of slope and corresponding critical slip surface. One of the main advantages of the FEM with reduced shear strength is that the safety factor emerges naturally from the analysis without the user having to commit to any particular form of the mechanism *a priori* (Griffiths & Lane 1999). Furthermore, it is possible for the FEM with reduced shear strength to evaluate the slope stability under a general framework even for the case of base stability of circular excavations (Cai & Ugai 2001).

A two-dimensional finite element program is used for the present analysis, where the return-mapping algorithm is used for stress integration, and the secant Newton method is used to accelerate the convergence of the modified Newton-Raphson scheme (Cai & Ugai 2001). The isoparametric elements with eight nodes are used to model the soil and wall elements. In order to obtain the precise results it is found that at least six rows of elements must be put below the bottom of the wall, where the soil failure should take place. The horizontal distance from the wall to the outer boundary of the excavation should be not less than at least  $2H$ . The vertical distance in the mesh under the base of excavation must be fine as possible which depends on the thickness of the clay under the base of excavation, for example the vertical distance is 0.25 m in the case of  $T = 3.0$  m, and 0.50 m in the case of  $T = 4.50$  m.

The reduced integration is used to avoid the numerical difficulties, known widely as 'locking', arising when modeling incompressible soft soils (Cai & Ugai 2001). The soil is modeled as linear elastic-perfectly plastic with the Mohr-Coulomb yield surface and the wall is assumed to behave linear elastically. The shear strength of the thin interface element was given 0.1 the shear strength of the clay. The excavated depth,  $H$ , of all excavations analyzed is 9m, and the other geometrical parameters are

changed case by case. The mechanical properties of the soft clay are shown in Table 1.

Table 1. Mechanical properties of the soft clay

| Parameter                                  | Value           |
|--|-----------------|
| Undrained shear strength, $s_u$ (kPa)      | 35.0            |
| Young's modulus, $E_u$ (kPa)               | $E_u = 250 s_u$ |
| Poisson's ratio, $\nu$                     | 0.49            |
| Unit weight, $\gamma$ (kN/m <sup>3</sup> ) | 20.0            |

### 3 UPPER BOUND ANALYSES

The closed equations considering embedment depth under the base of braced excavations has been proposed based on the upper bound analysis. The loads, determined by equating the external work to the internal rate of dissipation in an assumed deformation mode (or velocity field) that satisfies velocity boundary conditions and strain and velocity compatibility conditions. The dissipation of energy in plastic flow associated with such a field can be computed from the idealized stress/strain rate relation (or the so-called flow rule). If the soil layer of the thickness,  $D$ , below the excavation base acts as a load,  $\gamma D$ , and the wall is rigid, several upper bound solutions could be derived from the energy dissipation assumption. Three cases could be considered: (1) where no embedded depth of the wall and  $T \leq Tc$ , (2) where there are embedded depth of the wall and  $Tn > Tc$ , and (3) where there are embedded depth of the wall and  $Tn < Tc$ . The value of  $\gamma H/s_u$  in the upper bound analysis is equivalent to the  $Nc$ -value in the FE analysis.

### 4 RESULTS AND DISCUSSIONS

The base instability can be indicated using the normalized maximum rebounding displacement on the excavation base,  $\Delta$ ,

$$\Delta = \frac{\delta_{\max} E_u}{s_u (H + T)} \quad (1)$$

where  $\delta_{\max}$  is the maximum nodal displacement in the base of excavation. The location of this point is not fixed, but it depends on the geometry of the excavation. This point can be found at the middle of excavation if  $T \geq Tc$ ; otherwise, it is located near the wall. The normalized displacement,  $\Delta$ , increases with the reduction factor of the shear strength,  $F$ , and dramatically develops with  $F$  trending to the safety factor of the excavation bases, as indicated in Figure 2. This is similar to the results for two-dimensional excavations, reported by Smith & Ho (1992) and Goh (1994).

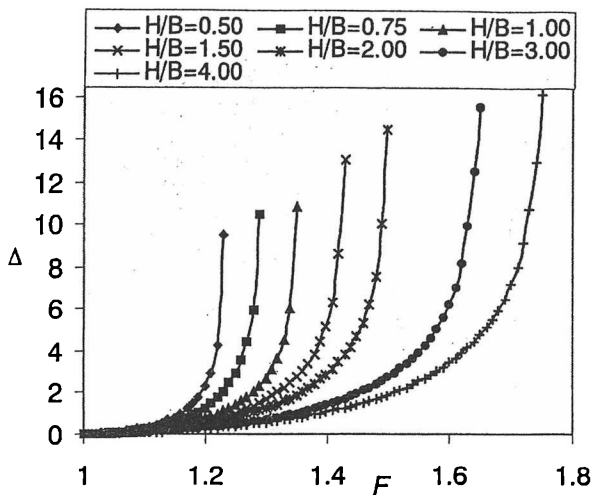


Figure 2. Normalized displacement versus shear strength reduction factor,  $F$  ( $D=0.0$ ).

#### 4.1 Effect of $H/B$ ( $D=0.0$ , $T \geq T_c$ )

The results of the FEM with reduced shear strength indicate that the location of hard stratum has influence on the  $N_c$ -value, when the thickness of the soft soil layer below the excavation base is less than the critical depth, i.e.  $T \leq T_c = B/\sqrt{2}$ . When  $T \geq T_c$  and  $D=0$ , the influence of  $H/B$  on the base stability is indicated in Figure 3, where the  $N_c$ -value is the same as that in Bjerrum & Eide's method, and is given by

$$N_c = Fs \gamma H / s_u \quad (2)$$

The  $N_c$ -value in Terzaghi's method for the excavations is given by

$$N_c = 5.7 + H/T \quad (3)$$

Another mechanism for velocity field leads to the following upper bound solution, which is also derived, based on the upper bound analysis, assuming a kinematically admissible velocity field.

$$N_c = 6.14 + H/\sqrt{2T} \quad (4)$$

In Equations (3) and (4),  $T$  must be taken equal to  $T_c$  in the case of  $T > T_c$ , and  $T$  is just its value if  $T \leq T_c$ . The  $N_c$ -value is a dimensionless coefficient depending on the geometry of the excavation.

From Figure 2 the factor of safety  $F_s$  can be obtained based on the FEM. The factor of safety is taken at which nodal displacements indicate a rapid increase in the deformation. By substituting the value of safety factor obtained from Figure 2 into Equation (2), the  $N_c$ -value can be obtained.

Figure 3 indicates that the  $N_c$ -value, predicted with the FEM with reduced shear strength, is close to Equation (3) for the shallow or wide excavation with  $H/B \leq 1.0$ . When  $H/B > 1.0$ , the  $N_c$ -value of the FEM increases with the ratio of  $H/B$  and are higher than Bjerrum & Eide's method. Also the  $N_c$ -value, predicted with the FEM is less than equation

(4) when  $H/B > 1.0$ . Also, from Figure 3 it can be seen that in the case of  $T/T_c = 2.0$  there is a little decrease in the safety factor which was not considered in both Terzaghi and Prandtl method's. From Figure 3 the FEM solutions give less safety factor than that obtained from the upper bound analysis.

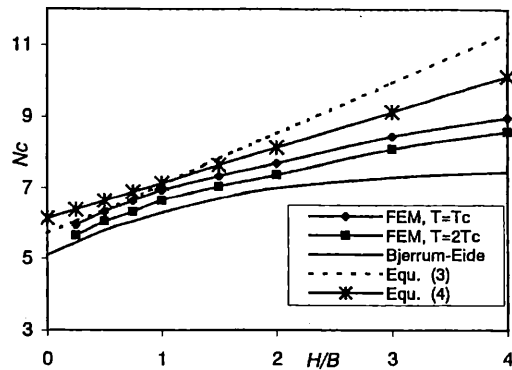


Figure 3. Effect of  $H/B$  on  $N_c$  value ( $T \geq T_c$  and  $D=0$ ).

The failure mechanism by the FEM can be indicated using nodal displacement vectors induced by the shear strength reduction just before the failure takes place. The failure mechanism for  $H/B = 1.0$  with  $T = T_c$  is shown in Figure 4.

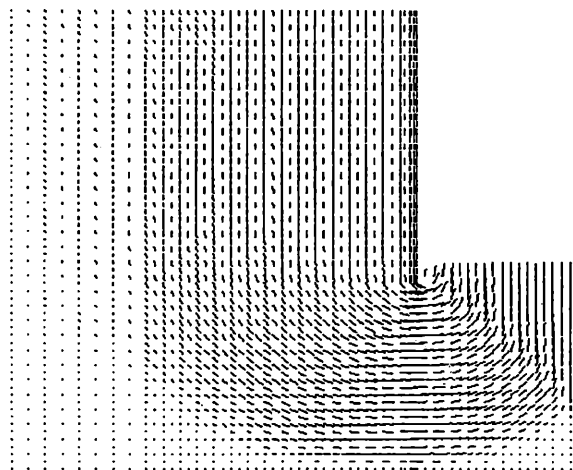


Figure 4. Nodal displacement vectors for  $H/B = 1.0$ ,  $D = 0.0$ , and  $T = T_c$ .

#### 4.2 Effect of $T/T_c$ ( $D=0.0$ )

In this section the effect of clay thickness under the excavation base is considered. It was found that it has influence on the stability of the base as shown in Figure 5. It can be concluded that the safety factor increases with decreasing the thickness of clay under the base of excavation.

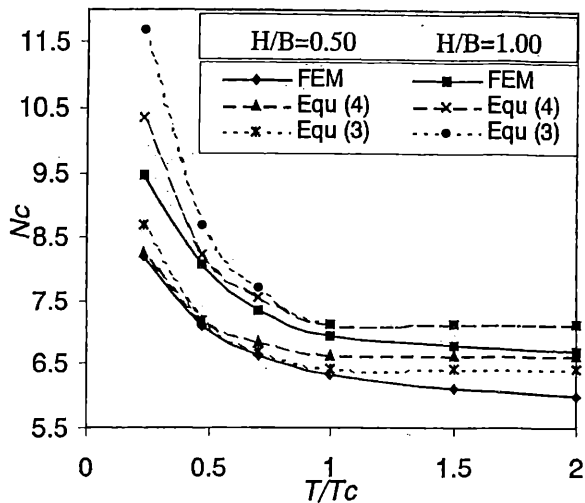


Figure 5. Influence of  $T/T_c$  on  $N_c$ -value ( $D=0$ ).

When  $T/T_c > 1.0$ , the increasing of clay depth will slightly reduce the  $N_c$ -value; however, the reduction of the  $N_c$ -value is smaller than 5% as shown in Figure 5. Figure 5 indicates that the presence of the hard stratum close to the excavation base increases the  $N_c$ -value when  $T/T_c < 1.0$ . This is because the size of the yielding zone is influenced, and the displacement of the soil beneath and around the excavation is restrained.

Figure 5 shows that the  $N_c$ -values of Equation (3) and Equation (4) are larger than that of the FEM with reduced shear strength.

Figure 6 shows the failure mechanism when  $H/B = 1.0$  and  $T/T_c = 0.24$ . The failure zone is restrained, and similar to that assumed by Terzaghi for the shallow or wide excavations with a limited thickness of the soft soil layer in the two-dimensional situations. This cannot be considered by Bjerrum & Eide's method.

#### 4.3 Effect of $T/T_c$ ( $D > 0.0$ )

The results of the FEM with reduced shear strength indicate that the thickness of the clay layer has influence on the  $N_c$ -values when  $T \leq T_c$ . Figure 7 shows the effect of the embedded depth. It indicates that the safety factor increases with increasing  $D/T_c$  in the case of  $T \leq T_c$ ; this is because the wall resists the movement of soil towards the base of excavation, which increases the safety factor. When  $T > T_c$ , the influence of  $D$  on  $F_s$  values is indicated in Figure 7. For clay extending to a considerable depth below the base of excavation the effect of increasing the embedded depth of the wall will result a marginal increase in safety factor. From Figure 8 it can be seen that, for clay that has bigger depth ( $T = 2T_c$ ) below the base of excavation, with increasing the embedded depth of the wall, the increasing of safety factor will be smaller than in the case of  $T \leq T_c$ . While in

the case of  $T > T_c$  the increase of embedded depth of the wall until  $D/T = 0.70$  has increased the safety factor with about 20% but in the case of  $T < T_c$  the increase in safety factor for  $D/T = 0.70$  is about more than 50%.

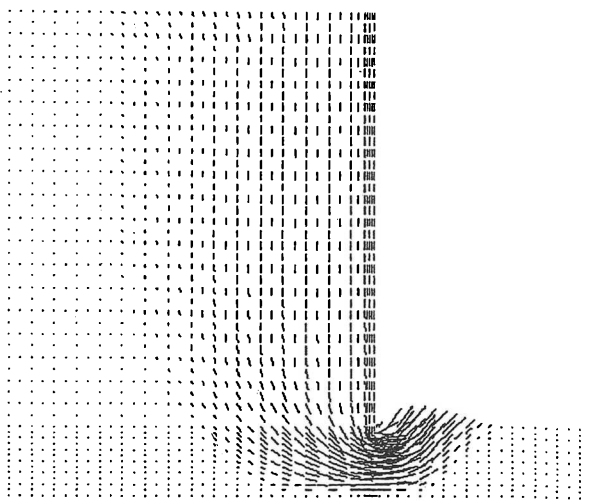


Figure 6. Nodal displacement vectors for  $D = 0.0$ ,  $H/B = 1.0$ , and  $T/T_c = 0.24$ .

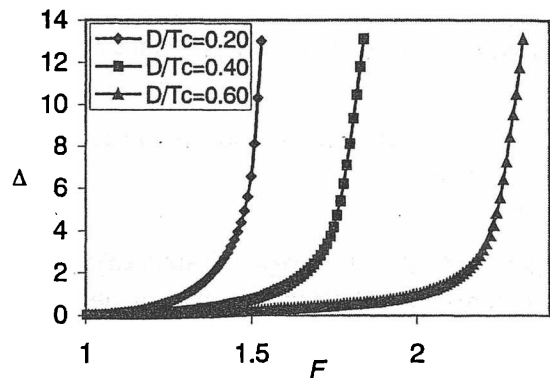


Figure 7. Effect of embedded depth ( $T = T_c$ ).

The reason why the increase in safety factor is small in the case of large clay thickness under the base of excavation and larger embedded wall depth is shown in Figures 9 and 10. The safety factors in these two cases are 1.58 and 1.75, respectively. From Figures 9 and 10 it can be concluded that, shorter embedded depth give higher resistance to soil movement. As shown in Figure 9, the relative nodal displacement at the end of the wall and the adjacent soil is large which means the wall give high resistance to the soil movement. But in the case of large embedded depth as shown in Figure 10, the relative nodal displacement at the end of the wall and the adjacent soil is small which means that the resistance of the wall to displacement with the soil is small.

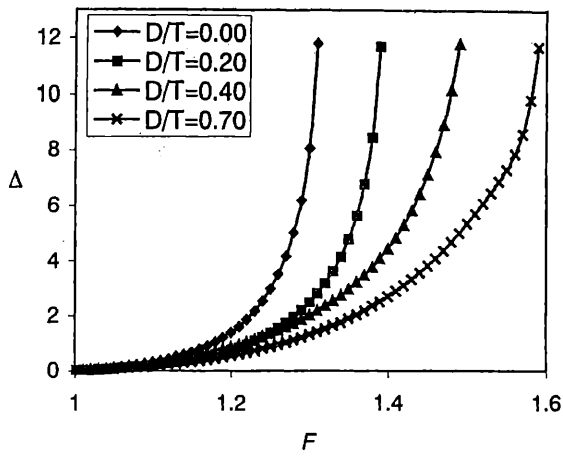


Figure 8. Effect of embedded depth on safety factor ( $T = 2T_c$ ).

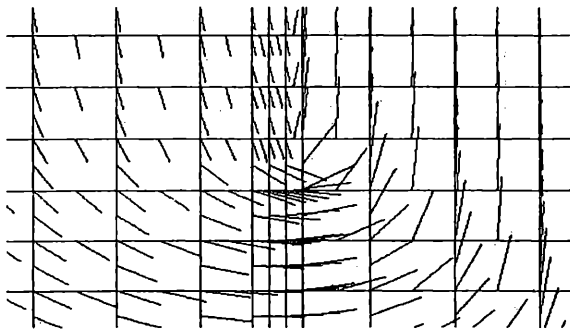


Figure 9. Nodal displacement vectors when  $H/B = 1.50$ ,  $D/T = 0.40$ , and  $T = 2T_c$  (local view at the end of the wall).

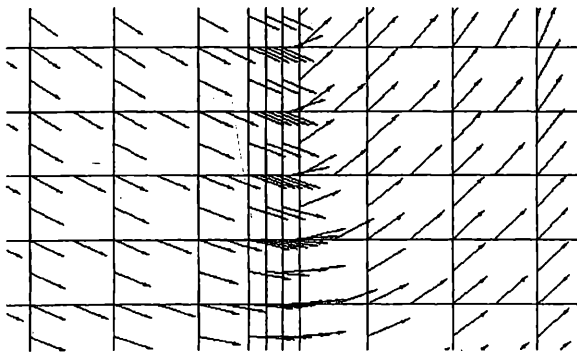


Figure 10. Nodal displacement vectors when  $H/B = 1.50$ ,  $D/T = 0.70$ , and  $T = 2T_c$  (local view at the end of the wall).

#### 4.4 Effect of $D$ and wall stiffness

From the analyses of effect of wall stiffness on safety factor, it can be noticed that, there are relation between the embedded depth and wall stiffness as shown in Figure 11. The safety factor increases with increasing the stiffness of the wall, which depends on the embedded length of the wall. The increase in  $F_s$  as  $D$  increases is likely to be because the wall

stiffness reduces the tendency of the clay behind the wall and adjacent to the base of excavation to be displaced toward the excavation.

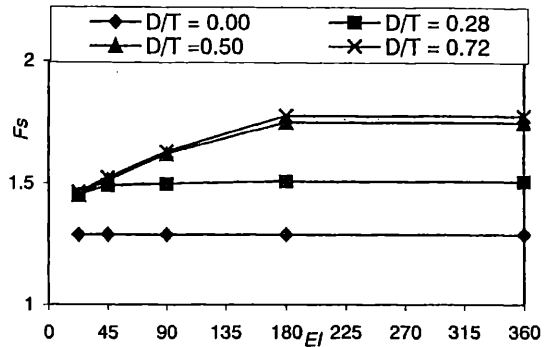


Figure 11. Effect of embedded depth and wall stiffness on safety factor when  $H/B = 0.75$  and  $T = T_c$ .

Also the relative nodal displacement for low rigidity wall and rigid wall are clear as shown in Figures 12 and 13. The calculated safety factors in these two cases are 1.53 and 1.74 respectively.

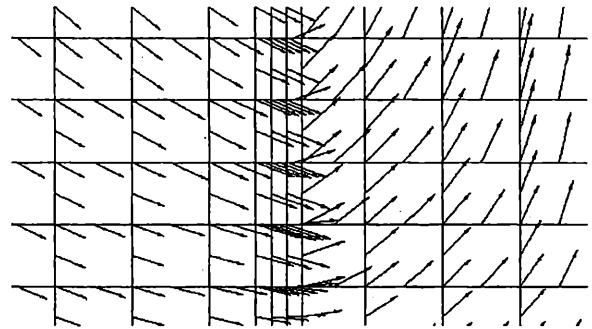


Figure 12. Nodal displacement vectors when  $H/B = 1.50$ ,  $D/T = 0.60$ ,  $T/T_c = 1.0$ , and  $EI = 45\text{MNm}^2$  (local view at the end of the wall).

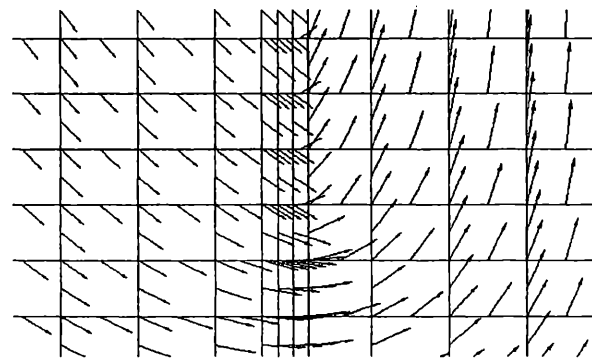


Figure 13. Nodal displacement vectors when  $H/B = 1.50$ ,  $D/T = 0.60$ ,  $T/T_c = 1.0$ , and  $EI = 360\text{MNm}^2$  (local view at the end of the wall).

## 5 CONCLUSIONS

The  $N_c$ -values of excavations are predicted using the FEM with reduced shear strength compared with the ones from the closed equations derived by the upper bound theorem. The influences of  $H/B$ ,  $T$ ,  $EI$  and  $D$  on the  $N_c$ -values of excavations are evaluated. As the results of the FEM with reduced shear strength, the following conclusions are obtained:

(1) The  $N_c$ -values of excavations increase almost linearly with  $H/B$  when  $H/B \leq 1.0$ , and slightly increase with  $H/B$  when  $H/B > 1.0$  under  $D = 0.0$

(2) The presence of the hard stratum close to the base of excavation ( $T < T_c$ ) increases significantly the  $N_c$ -value of excavations under  $D = 0.0$ .

(3) The influence of  $D$  on the  $N_c$ -values of excavations depends on the wall stiffness.

(4) To obtain good result in the case of using FEM for two-dimensional base stability, the following factors must be considered: (i) The horizontal distance from the wall to the outer border of the excavation is at least  $2H$ ; (ii) Make the vertical distance in the mesh under the base of excavation as fine as possible; (iii) The minimum number of row in the mesh under the wall is not less than six rows.

## REFERENCES

- Bjerrum, L., and Eide, O. (1956). "Stability of strutted excavations in clay." *Geotechnique*, 6(1), 32-47.
- Cai, F., and Ugai, K. (2000). "Numerical analysis of the stability of a slope reinforced with piles." *Soils and Foundations*, 40(1), 73-84.
- Cai, F., and Ugai, K. (2001). "Base stability of circular excavation in soft clay estimated by FEM." *Proceeding of the Third International Conference on Soft Soil Engineering*, Hong Kong, 305-310.
- Goh, A. T. C. (1994). "Estimating basal-heave stability for braced excavations in soft clay." *J. Geotech. Engrg.*, ASCE, 120(8), 1430-1436.
- Griffiths, D. V., and Lane, P. A. (1999). "Slope stability analysis by finite elements." *Geotechnique*, 49(3), 387-403.
- Manzari, W. T., and Nour, M. A. (2000). "Significance of soil dilatancy in slope stability analysis." *J. Geotech. And Geoenviron. Engrg.*, ASCE, 126(1), 75-80.
- Matsui, T., and San, K. C. (1992). "Finite element slope stability analysis by shear strength reduction technique." *Soils and Foundations*, 32(1), 59-70.
- Smith, I. M., and Ho, D. K. H. (1992). "Influence of construction technique on the performance of a braced excavation in marine clay." *Int. J. Numer. Anal. Meth. Geomech.*, 16(12), 845-868.
- Terzaghi, K. (1943). *Theoretical soil mechanics*. Wiley, New York.
- Ugai, K. (1989). "A method of calculation of global safety factor of slopes by elasto-plastic FEM." *Soils and Foundations*, 29(2), 190-195 (in Japanese).
- Ugai, K., and Leshchinsky, D. (1995). "Three-dimensional limit equilibrium and finite element analyses: a comparison of results." *Soils and Foundations*, 35(4), 1-7.
- Zienkiewicz, O. C., Humpheson, C., and Lewis, R. W. (1975). "Associated and non-associated visco-plasticity and plasticity in soil mechanics." *Geotechnique*, 25(4), 671-689.